

# ISOCURVATURE FORECASTS FOR PLANCK, CMB S4, AND PIXIE, AND MAYBE CONSTRAINTS FOR ACTPOL

ZACK LI AND JO DUNKLEY

Astrophysical Sciences, Princeton University, Princeton NJ 08544

(Dated: April 30, 2017)

*Draft version April 30, 2017*

## ABSTRACT

We provide forecasts of cold dark matter isocurvature (CDI) constraints for combinations of Planck, CMB S4, and PIXIE. Using MCMC methods on fiducial power spectra, we find substantial improvements in the measurement of the large scale isocurvature power.

### 1. INTRODUCTION

The primordial cosmological perturbations are primarily adiabatic fluctuations, which come from a spatially uniform equation of state and initial velocity field and lock together the density perturbations of the different components (Planck Collaboration et al. 2014). Several scenarios allow for spatially varying equations of state or initial velocity fields, producing isocurvature perturbations.

**Motivations.** Inflation with a single scalar field and slow-roll initial conditions excites only adiabatic perturbations. However, multiple field inflation can produce an isocurvature spectrum as well as an adiabatic spectrum, with possible correlations between the two (Langlois 1999). Commonly studied isocurvature perturbations arise from variations between photon density, cold dark matter (CDM) density, neutrino density (NID), and neutrino velocity (NIV). Quantum fluctuations can also lead to the curvaton scenario, which also generating isocurvature perturbations correlated with the adiabatic modes (Baumann et al. 2009). Some string theory axions can also carry isocurvature fluctuations from quantum fluctuations, with an axion decay to dark matter leading to uncorrelated adiabatic and CDM isocurvature perturbations.

In this paper we forecast constraints on CDM isocurvature using MCMC on fiducial power spectra and simulations of future CMB experiments. The CDM isocurvature contribution to TT, TE, and EE power spectra is out of phase with the adiabatic perturbations in  $C_l$ , so improvements in CMB polarization measurements can considerably improve upon current constraints (see Section X.X). We simulate combinations of Planck, CMB S4, and PIXIE. **Should I cite each experiment here?**

**Current Constraints.** Current measurements of isocurvature are consistent with fully adiabatic primordial density fluctuations. Previous constraints on isocurvature constraints have come from precision measurements of the CMB power spectrum, with WMAP (Moodley et al. 2004) and Planck (Planck Collaboration et al. 2014). Joint WMAP and BAO constraints on fully uncorrelated and anticorrelated modes put upper bounds on the isocurvature at less than a percent (Hinshaw et al. 2013). **Should I include actual numbers?** The tightest constraints on isocurvature (Planck Collaboration et al. 2016a) currently limit the amplitude of CDM isocurvature fluctuations to a few percent at large scales

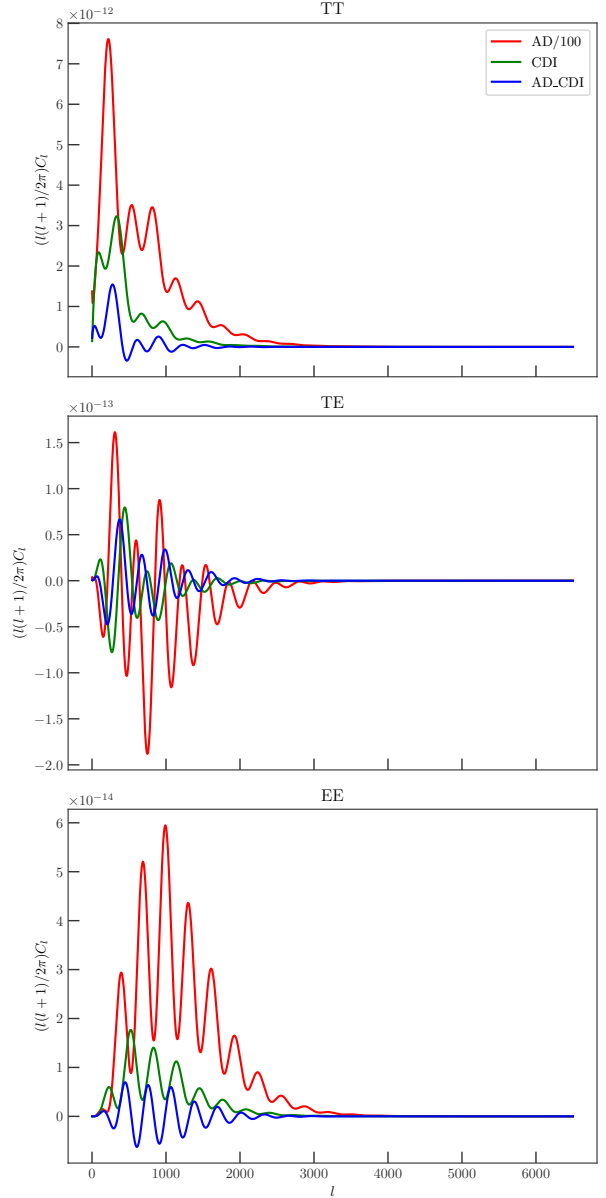


FIG. 1.— Scaled adiabatic and isocurvature contributions to  $\mathcal{D}_l$  for a model with nonzero isocurvature consistent with the Planck measurements. **overplot ACTPol error bars?**

( $k = 0.002 \text{ Mpc}^{-1}$ ), and 30-50% at small scales ( $k = 0.1 \text{ Mpc}^{-1}$ ). These use polarization measurements over the Planck range of  $l = 2 - 2508$  for TT and  $2 - 1996$  for TE and EE.

**Recent Forecasting Papers.** Bucher et al. (2001) forecasted isocurvature constraints for Planck, the current best constraints on isocurvature using a Fisher matrix analysis. These forecasts have been shown to be consistent with actual measurements. Simulated forecasts for only CMB-S4 (Abazajian et al. 2016) predict increases in sensitivity by a factor of 3-6 over Planck. For the curvature scenario, Smith & Grin (2016) make forecasts using an MCMC analysis for a cosmic-variance limited experiment. Muya Kasanda & Moodley (2014) make isocurvature forecasts for the PRISM experiment and investigate the effects of the CMB lensing potential in-depth.

## 2. METHODS

### 2.1. Perturbations and Power Spectra

**todo: heuristic description of isocurvature effects on CMB power spectra. maybe I include something like the  $dD_l/dP_{II}^j$  plots.**

Gaussian fluctuations for a general cosmological perturbation are described by a matrix of power spectra, referring to correlations and amplitudes. In this paper, we only consider primordial CDM isocurvature, so the matrix is  $2 \times 2$  where  $\mathcal{P}_{II}(k)$  is the power spectrum of  $\delta\rho_{\text{CDM}}/\rho_{\text{CDM}}$ , with  $\rho_{\text{CDM}} = n_c/n_\gamma$ , the ratio of primordial CDM to photon number densities.

$$\mathcal{P}(k) = \begin{pmatrix} \mathcal{P}_{\mathcal{R}\mathcal{R}}(k) & \mathcal{P}_{\mathcal{R}\mathcal{I}}(k) \\ \mathcal{P}_{\mathcal{R}\mathcal{I}}(k) & \mathcal{P}_{\mathcal{I}\mathcal{I}}(k) \end{pmatrix} \quad (1)$$

Following Planck Collaboration et al. (2016a), we parametrize  $\mathcal{P}_{\mathcal{R}\mathcal{R}}$ ,  $\mathcal{P}_{\mathcal{R}\mathcal{I}}$ , and  $\mathcal{P}_{\mathcal{I}\mathcal{I}}$  by choosing the power at two scales,  $k_1 = 0.002 \text{ Mpc}^{-1}$  and  $k_2 = 0.100 \text{ Mpc}^{-1}$  and interpolating geometrically,

$$\mathcal{P}_{ab}(k) = \exp \left[ \left( \frac{\ln(k) - \ln(k_2)}{\ln(k_1) - \ln(k_2)} \right) \ln(\mathcal{P}_{ab}^1) + \left( \frac{\ln(k) - \ln(k_1)}{\ln(k_2) - \ln(k_1)} \right) \ln(\mathcal{P}_{ab}^2) \right].$$

Thus one can recover the tilt by computing the log-log slope,

$$n_{ab} = \frac{\log(\mathcal{P}_{ab}^2/\mathcal{P}_{ab}^1)}{\log(k_2/k_1)}. \quad (2)$$

For a set of the standard cosmological parameters with the additional isocurvature parameters, we compute a theoretical power spectrum with CLASS, a fast Boltzmann code written in C (citation). The adiabatic and isocurvature are contained in three functions,  $\mathcal{P}_{\mathcal{R}\mathcal{R}}(k)$ ,  $\mathcal{P}_{\mathcal{I}\mathcal{I}}(k)$ , and  $\mathcal{P}_{\mathcal{R}\mathcal{I}}(k)$ , the curvature, isocurvature, and cross-correlation power spectra, respectively (cite Planck 2015 XX). We use the same uniform priors as Planck,

$$\mathcal{P}_{\mathcal{R}\mathcal{R}}^{(1)}, \mathcal{P}_{\mathcal{R}\mathcal{R}}^{(2)} \in (10^{-9}, 10^{-8}), \quad (3)$$

$$\mathcal{P}_{\mathcal{I}\mathcal{I}}^{(1)}, \mathcal{P}_{\mathcal{I}\mathcal{I}}^{(2)} \in (0, 10^{-8}), \quad (4)$$

$$\mathcal{P}_{\mathcal{R}\mathcal{I}}^{(1)} \in (-10^{-8}, 10^{-8}). \quad (5)$$

We follow Planck 2015 XX's convention of only sampling over  $\mathcal{P}_{\mathcal{R}\mathcal{I}}^{(1)}$  and fixing  $\mathcal{P}_{\mathcal{R}\mathcal{I}}^{(2)}$  by restricting the correlation fraction to be scale-independent,

$$\cos \Delta_{ab} = \frac{\mathcal{P}_{ab}}{(\mathcal{P}_{aa}\mathcal{P}_{bb})^{1/2}} \in (-1, 1), \quad (6)$$

so that

$$\mathcal{P}_{ab}^{(2)} = \mathcal{P}_{ab}^{(1)} \frac{(\mathcal{P}_{aa}^{(2)}\mathcal{P}_{bb}^{(2)})^{1/2}}{(\mathcal{P}_{aa}^{(1)}\mathcal{P}_{bb}^{(1)})^{1/2}}. \quad (7)$$

We also present the results in terms of derived parameters following Planck Collaboration et al. (2016a), defining the primordial isocurvature fraction as

$$\beta_{\text{iso}}(k) = \frac{\mathcal{P}_{\mathcal{I}\mathcal{I}}(k)}{\mathcal{P}_{\mathcal{R}\mathcal{R}}(k) + \mathcal{P}_{\mathcal{I}\mathcal{I}}(k)}. \quad (8)$$

Then we sample over the  $\Lambda\text{CDM}$  scenario, but replace  $A_s$  and  $n_s$  with  $\mathcal{P}_{\mathcal{R}\mathcal{R}}^{(1)}$ ,  $\mathcal{P}_{\mathcal{R}\mathcal{R}}^{(2)}$  and add the three isocurvature parameters  $\mathcal{P}_{\mathcal{I}\mathcal{I}}^{(1)}$ ,  $\mathcal{P}_{\mathcal{I}\mathcal{I}}^{(2)}$ ,  $\mathcal{P}_{\mathcal{R}\mathcal{I}}^{(1)}$ .

$$\{\Omega_b h^2, \Omega_c h^2, \theta_A, \tau_{\text{reio}}, \mathcal{P}_{\mathcal{R}\mathcal{R}}^{(1)}, \mathcal{P}_{\mathcal{R}\mathcal{R}}^{(2)} \quad (9)$$

$$\mathcal{P}_{\mathcal{I}\mathcal{I}}^{(1)}, \mathcal{P}_{\mathcal{I}\mathcal{I}}^{(2)}, \mathcal{P}_{\mathcal{R}\mathcal{I}}^{(1)} \} \quad (10)$$

### 2.2. Forecasting

We create mock likelihoods following Perotto et al. (2006), in which for each experiment we are using in our forecasts, we estimate an  $l$ -range,  $f_{\text{sky}}$ , beam width  $\theta_{\text{fwhm}}$ , temperature noise  $\sigma_T$ , and polarization noise  $\sigma_P$ . Then we have, for  $X, Y \in \{T, E, B\}$  (Perotto et al. 2006),

$$\mathbf{N}_l^{XY} = \delta_{XY} \theta_{\text{fwhm}}^2 \sigma_X^2 \exp \left[ l(l+1) \frac{\theta_{\text{fwhm}}}{8 \ln 2} \right] \quad (11)$$

The parameters we use for each experiment are in Table 1.

For CMB-S4, we also include a multiplicative factor for atmospheric noise, in the form of a fitting function with  $l_{\text{knee}} = 330$ ,  $\alpha = -3.8$ ,

$$N_l = N_0 \left( 1 + \left( \frac{l}{l_{\text{knee}}} \right)^\alpha \right) \quad (12)$$

We then use this  $N_l$  with a fiducial power spectrum generated in CLASS with the Planck 2015 cosmological parameters (Planck Collaboration et al. 2016b). We investigate both a fiducial spectrum with zero isocurvature, and one a relatively extreme model which is still consistent with the Planck constraints.

We find constraints for the isocurvature parameters using these likelihood parameters and Markov Chain Monte Carlo (MCMC) sampling. We use Monte Python, a Python-based implementation of Metropolis-Hastings and interface for cosmological likelihoods. We use six different combinations of experiments.

1. Planck TT ( $2 \leq l \leq 2500$ ),  
Planck TEB ( $2 \leq l \leq 30$ ).
2. Planck TEB ( $2 \leq l \leq 2500$ ).
3. Planck TEB ( $2 \leq l \leq 30$ ),  
CMB-S4 ( $30 < l \leq 3000$ ).

TABLE 1  
FORECASTING PARAMETERS

Experiment	$l_{min} - l_{max}$	$f_{sky}$	$\theta_{FWHM}$	$\sigma_T$ ( $\mu K$ arcmin)	$\sigma_P$ ( $\mu K$ arcmin)
CMB-S4	30-3000	0.40	3.0	1.0	1.4
PIXIE	2 - 150	0.8	120	2.9	4.0
Planck 2015 high-l + pol	2 - 2500	0.65	10,7.1,5.0	65.0, 43.0, 66.0	103.0, 81.0, 134.0

NOTE. — Noise parameters for CMB-S4 (Abazajian et al. 2016), PIXIE (FIND CITATION), and Planck + Planck Polarization (Planck Collaboration et al. 2016a). The three Planck noise levels come from three channels at 70, 100 and 143 GHz respectively.

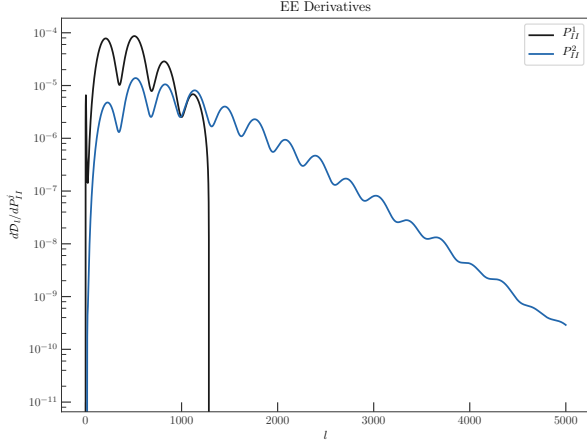


FIG. 2.— A measurement of the impact of the two isocurvature powers  $\mathcal{P}_{\mathcal{I}\mathcal{I}}^1$  and  $\mathcal{P}_{\mathcal{I}\mathcal{I}}^2$ , by taking the derivative of  $\mathcal{D}_l$  with respect to  $\mathcal{P}_{\mathcal{I}\mathcal{I}}^i$ , for a model with nonzero isocurvature consistent with the Planck measurements.

4. PIXIE over ( $2 \leq l \leq 150$ ),  
Planck TEB ( $150 < l \leq 2500$ ).
5. PIXIE over ( $2 \leq l \leq 150$ ),  
CMB-S4 ( $150 < l \leq 2500$ ).

### 2.3. ACTPol Likelihood

We use the same methods as in Louis et al. 2016 for the ACT likelihood, marginalizing the ACTPol spectrum from  $350 < l < 4000$  to construct a Gaussian likelihood function with an overall calibration parameter. We produce our parameter constraints by summing this with

the Planck 2015 log-likelihood. We use the public CMB-marginalized 'plik-lite' Planck 2015 likelihood which uses TT for  $30 \leq l \leq 2508$ , a likelihood generated from CMB lensing, and a joint TT, EE, BB, and TE likelihood for the range  $2 \leq l < 30$ .

$$-2 \ln L = -2 \ln L(\text{ACTPol}) \quad (13)$$

$$-2 \ln L(\text{Planck TT}_{30 < l < 2508}) \quad (14)$$

$$-2 \ln L(\text{Planck TEB}_{2 \leq l < 30}) \quad (15)$$

$$-2 \ln L(\text{Planck Lensing}) \quad (16)$$

In addition to the  $\Lambda$ CDM and isocurvature parameters, we need two nuisance parameters coming from the normalizations of the two instruments we use data from (Planck and ACT),

$$\{A_{\text{planck}}, Y_p\}. \quad (17)$$

### 3. RESULTS

The bestfit values are  $\mathcal{P}_{\mathcal{I}\mathcal{I}}^1 = \text{something}$ ,  $\mathcal{P}_{\mathcal{I}\mathcal{I}}^2 = \text{something}$ .

- Write about triangle plot
- Write about derived parameters
- Make a table summarizing various parameters with errors

### 4. CONCLUSION

### APPENDIX

#### comparing the fiducial power spectrum Planck parameter estimates with real Planck

### REFERENCES

- Abazajian, K. N., Adshead, P., Ahmed, Z., Allen, S. W., Alonso, D., Arnold, K. S., Baccigalupi, C., Bartlett, J. G., Battaglia, N., Benson, B. A., Bischoff, C. A., Borrill, J., Buza, V., Calabrese, E., Caldwell, R., Carlstrom, J. E., Chang, C. L., Crawford, T. M., Cyr-Racine, F.-Y., De Bernardis, F., de Haan, T., di Serego Alighieri, S., Dunkley, J., Dvorkin, C., Errard, J., Fabbian, G., Feeney, S., Ferraro, S., Filippini, J. P., Flauger, R., Fuller, G. M., Gluscevic, V., Green, D., Grin, D., Grohs, E., Henning, J. W., Hill, J. C., Hlozek, R., Holder, G., Holzappel, W., Hu, W., Hufferberger, K. M., Keskitalo, R., Knox, L., Kosowsky, A., Kovac, J., Kovetz, E. D., Kuo, C.-L., Kusaka, A., Le Jeune, M., Lee, A. T., Lilley, M., Loverde, M., Madhavacheril, M. S., Mantz, A., Marsh, D. J. E., McMahon, J., Meerburg, P. D., Meyers, J., Miller, A. D., Munoz, J. B., Nguyen, H. N., Niemack, M. D., Peloso, M., Peloton, J., Pogorian, L., Pryke, C., Raveri, M., Reichardt, C. L., Rocha, G., Rotti, A., Schaan, E., Schmittfull, M. M., Scott, D., Sehgal, N., Shandera, S., Sherwin, B. D., Smith, T. L., Sorbo, L., Starkman, G. D., Story, K. T., van Engelen, A., Vieira, J. D., Watson, S., Whitehorn, N., & Kimmy Wu, W. L. 2016. ArXiv
- Baumann, D., Jackson, M. G., Adshead, P., Amblard, A., Ashoorioon, A., Bartolo, N., Bean, R., Beltrán, M., de Bernardis, F., Bird, S., Chen, X., Chung, D. J. H., Colombo, L., Cooray, A., Creminelli, P., Dodelson, S., Dunkley, J., Dvorkin, C., Easther, R., Finelli, F., Flauger, R., Hertzberg, M. P., Jones-Smith, K., Kachru, S., Kadota, K., Khoury, J., Kinney, W. H., Komatsu, E., Krauss, L. M., Lesgourgues, J., Liddle, A., Liguori, M., Lim, E., Linde, A., Matarrese, S., Mathur, H., McAllister, L., Melchiorri, A., Nicolis, A., Pagano, L., Peiris, H. V., Peloso, M., Pogorian, L., Pierpaoli, E., Riotto, A., Seljak, U., Senatore, L., Shandera, S., Silverstein, E., Smith, T., Vaudrevange, P., Verde, L., Wandelt, B., Wands, D., Watson, S., Wyman, M., Yadav, A., Valkenburg, W., & Zaldarriaga, M. 2009, 1141, 10

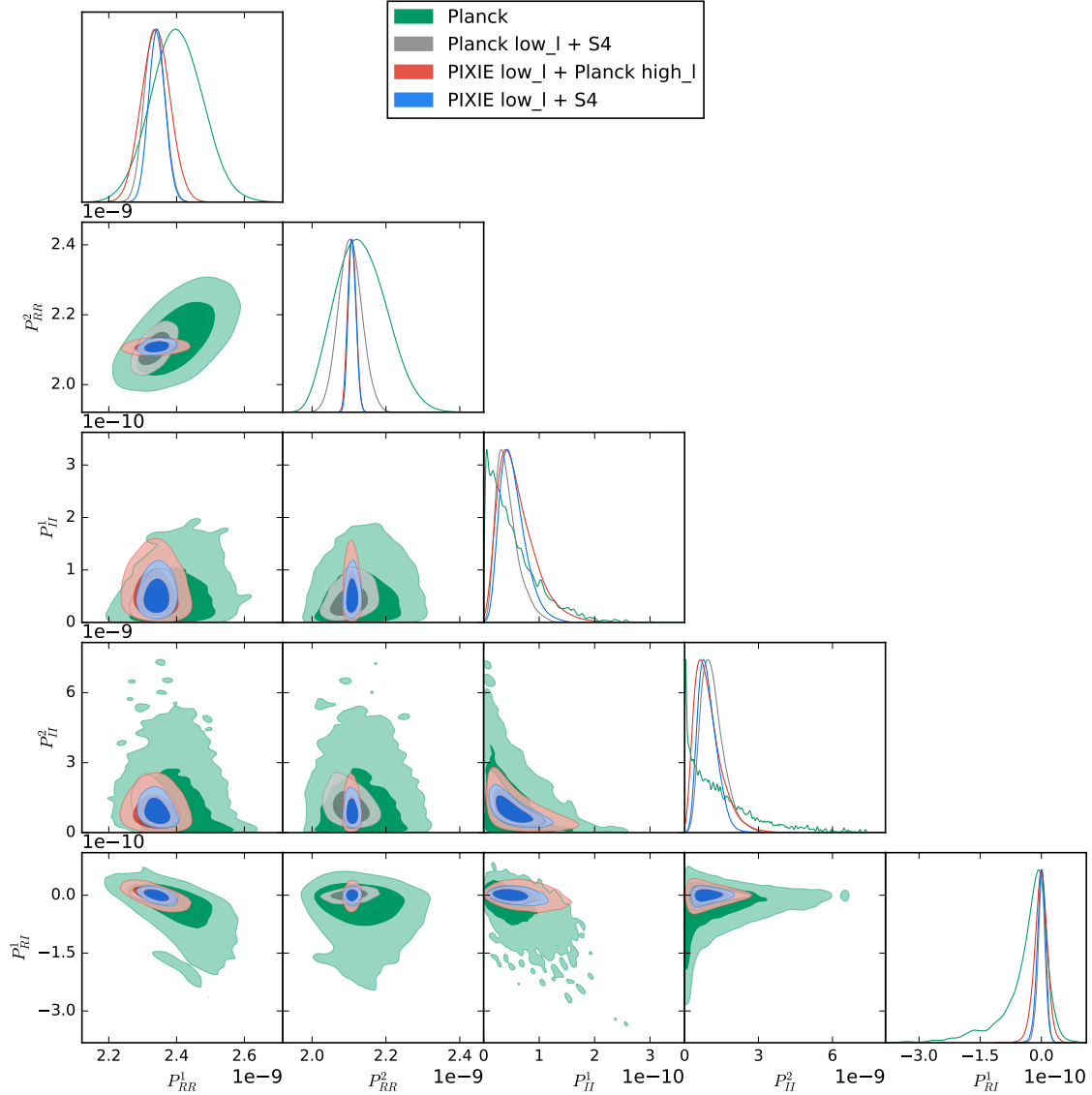


FIG. 3.— Isocurvature constraints for future CMB experiments.

Bucher, M., Moodley, K., & Turok, N. 2001, Physical Review Letters, 87, 191301  
 Hinshaw, G., Larson, D., Komatsu, E., Spergel, D. N., Bennett, C. L., Dunkley, J., Nolte, M. R., Halpern, M., Hill, R. S., Odegard, N., Page, L., Smith, K. M., Weiland, J. L., Gold, B., Jarosik, N., Kogut, A., Limon, M., Meyer, S. S., Tucker, G. S., Wollack, E., & Wright, E. L. 2013, ApJS, 208, 19  
 Langlois, D. 1999, Phys. Rev. D, 59, 123512  
 Moodley, K., Bucher, M., Dunkley, J., Ferreira, P. G., & Skordis, C. 2004, Phys. Rev. D, 70, 103520  
 Muya Kasanda, S. & Moodley, K. 2014, J. Cosmology Astropart. Phys., 12, 041  
 Perotto, L., Lesgourgues, J., Hannestad, S., Tu, H., & Y Y Wong, Y. 2006, J. Cosmology Astropart. Phys., 10, 013

Planck Collaboration, Ade, P. A. R., Aghanim, N., Armitage-Caplan, C., Arnaud, M., Ashdown, M., Atrio-Barandela, F., Aumont, J., Baccigalupi, C., Banday, A. J., & et al. 2014, A&A, 571, A16  
 Planck Collaboration, Ade, P. A. R., Aghanim, N., Arnaud, M., Arroja, F., Ashdown, M., Aumont, J., Baccigalupi, C., Ballardini, M., Banday, A. J., & et al. 2016a, A&A, 594, A20  
 Planck Collaboration, Ade, P. A. R., Aghanim, N., Arnaud, M., Ashdown, M., Aumont, J., Baccigalupi, C., Banday, A. J., Barreiro, R. B., Bartlett, J. G., & et al. 2016b, A&A, 594, A13  
 Smith, T. L. & Grin, D. 2016, Phys. Rev. D, 94, 103517

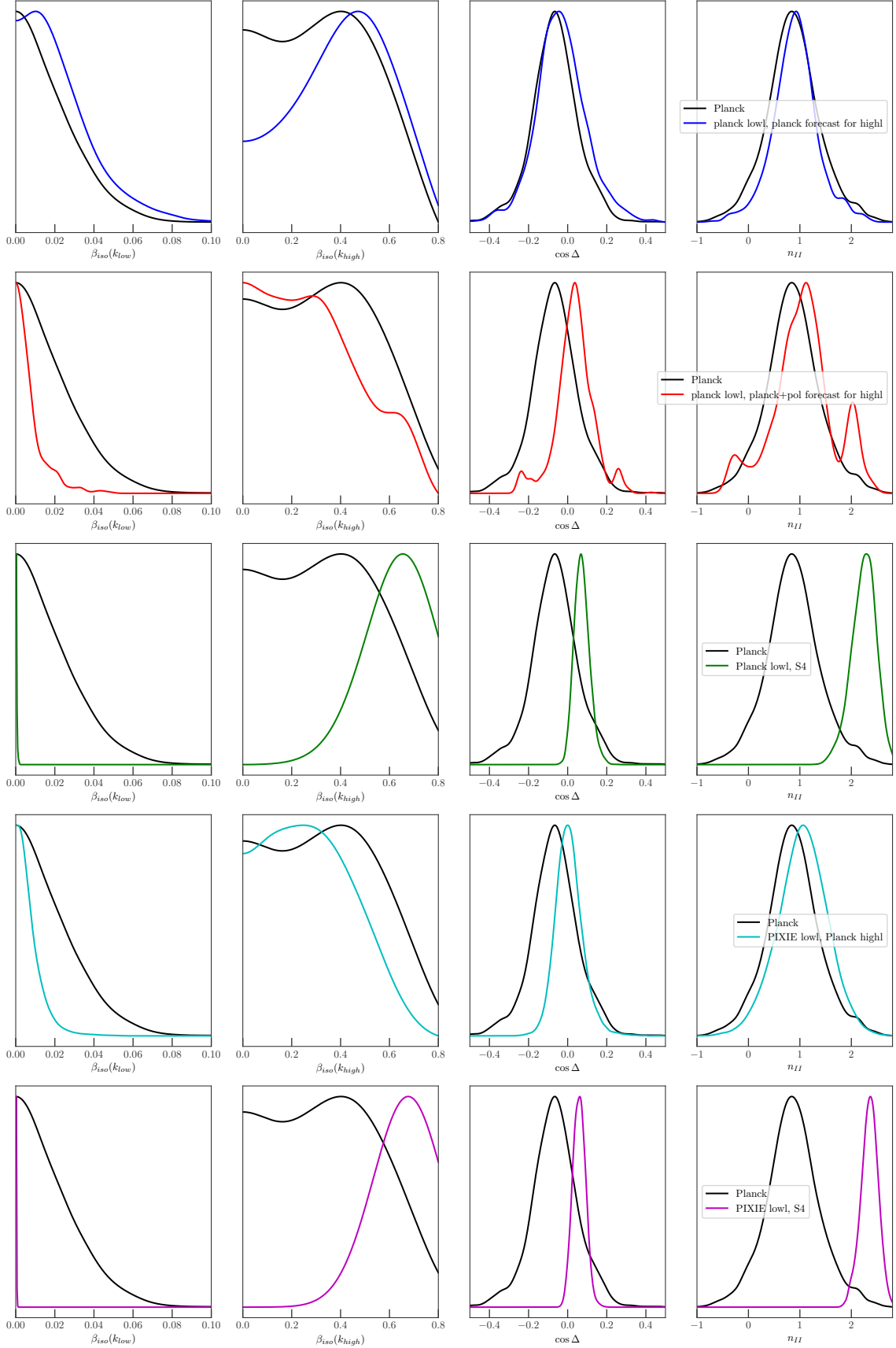


FIG. 4.— Derived parameter estimates for future CMB experiments.